Aalto University

OPEN ACCESS

This is an electronic reprint of the original article.
This reprint may differ from the original in pagination and typographic detail.

Brange, Fredrik; Prech, Kacper; Flindt, Christian

# Dynamic Cooper Pair Splitter

*Published in:*
Physical Review Letters

*DOI:*
10.1103/PhysRevLett.127.237701

Published: 03/12/2021

*Document Version*
Publisher's PDF, also known as Version of record

*Please cite the original version:*
Brange, F., Prech, K., & Flindt, C. (2021). Dynamic Cooper Pair Splitter. *Physical Review Letters*, *127*(23), 1-7. Article 237701. https://doi.org/10.1103/PhysRevLett.127.237701

This material is protected by copyright and other intellectual property rights, and duplication or sale of all or part of any of the repository collections is not permitted, except that material may be duplicated by you for your research use or educational purposes in electronic or print form. You must obtain permission for any other use. Electronic or print copies may not be offered, whether for sale or otherwise to anyone who is not an authorised user.

# Dynamic Cooper Pair Splitter

Fredrik Brange,[1] Kacper Prech,[1,2] and Christian Flindt[1]
[1]Department of Applied Physics, Aalto University, 00076 Aalto, Finland
[2]School of Physics and Astronomy, University of Glasgow, Glasgow G12 8QQ, United Kingdom

(Received 9 February 2021; accepted 8 November 2021; published 1 December 2021)

Cooper pair splitters are promising candidates for generating spin-entangled electrons. However, the splitting of Cooper pairs is a random and noisy process, which hinders further synchronized operations on the entangled electrons. To circumvent this problem, we here propose and analyze a dynamic Cooper pair splitter that produces a noiseless and regular flow of spin-entangled electrons. The Cooper pair splitter is based on a superconductor coupled to quantum dots, whose energy levels are tuned in and out of resonance to control the splitting process. We identify the optimal operating conditions for which exactly one Cooper pair is split per period of the external drive and the flow of entangled electrons becomes noiseless. To characterize the regularity of the Cooper pair splitter in the time domain, we analyze the $g^{(2)}$ function of the output currents and the distribution of waiting times between split Cooper pairs. Our proposal is feasible using current technology, and it paves the way for dynamic quantum information processing with spin-entangled electrons.

DOI: 10.1103/PhysRevLett.127.237701

*Introduction.*—Superconductors are natural sources of entangled particles [1]. By splitting the Cooper pairs in a superconductor into different normal-state leads, spin entanglement between spatially separated electrons can be achieved [2,3]. Cooper pair splitters have been realized in several types of solid-state architectures [4–20], for instance, using quantum dots [6,9,11], carbon nanotubes [7], or graphene [15,16,18,19]. Experimentally, the splitting process has been observed by measuring the nonlocal conductance or the noise [8,12] and recently using single-electron detectors [20]. However, with static voltages, the generation of spin-entangled electrons is a random and noisy process, which offers little control over the regularity and the timing of the Cooper pair splitting.

In parallel with these developments, single-electron emitters have emerged as accurate sources of noiseless currents [21–29]. By applying periodic gate or bias voltages to a nanoscale structure, such as a quantum dot [26–29], a mesocopic capacitor [22,23], or an Ohmic contact [24,25], single electrons can be periodically emitted into a ballistic conductor, leading to an electric current given by the driving frequency times the electron charge [30]. While experiments so far have mainly focused on dynamic sources that emit a single electron per cycle, theoretical works have explored the dynamic generation of more complex quantum states of entangled electrons in normal metals [31–34]. On the other hand, the concept of controlling the splitting of Cooper pairs with time-dependent driving fields has not been considered before; however, given the very recent experimental progress in the field [18–20], such ideas are finally within reach.

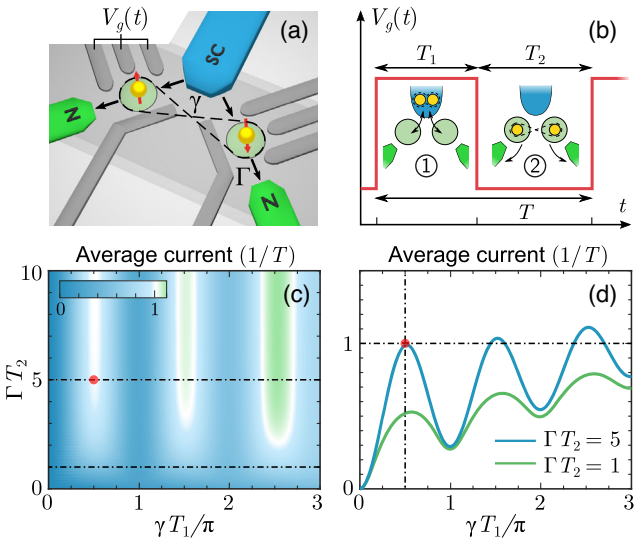


FIG. 1. Dynamic Cooper pair splitter. (a) The Cooper pair splitter consists of two quantum dots (light green) coupled to a superconductor (SC, blue) and two normal-metal drains ($N$, green). The splitting of Cooper pairs is controlled with the time-dependent gate voltage $V_g(t)$. (b) In phase 1 of the periodic driving protocol, Cooper pair splitting is tuned into resonance for the time $T_1$, so that a split Cooper pair tunnels into the dots (see insets). In phase 2, Cooper pair splitting is off resonance for the time $T_2$, and the electrons may escape via the drains. (c),(d) Average current in the drains as a function of $T_1$ and $T_2$ for $\Gamma = 0.1\gamma$, $\kappa = \gamma$, $\delta = 100\kappa$, with $\varepsilon = 0$ in phase 1 and $\varepsilon = 100\gamma$ in phase 2 (see main text for definitions). For the optimal conditions, $\gamma T_1 = \pi/2$, and $\Gamma T_2 = 5$, shown with a red dot, one Cooper pair is split per period of the drive.

 © 2021 American Physical Society

In this Letter, we propose and analyze a dynamic Cooper pair splitter that can deliver a noiseless and regular stream of spin-entangled electrons. Specifically, we show how the splitting of Cooper pairs can be controlled by applying time-dependent gate voltages to two quantum dots that are connected to a superconductor. We evaluate the average current and the fluctuations in the output leads and identify the optimal operating conditions for the dynamic Cooper pair splitter to produce a noiseless and regular current. Our proposal seems feasible in the light of recent experimental advances, and it may be realized using current technology.

*Dynamic Cooper pair splitter.*—Figure 1(a) shows our dynamic Cooper pair splitter consisting of a superconductor coupled to two single-level quantum dots. Cooper pairs from the superconductor are split between the dots due to strong on-site Coulomb interactions, which prevent each dot from being doubly occupied. Electrons on the dots are collected in separate normal-metal drain electrodes. Importantly for our proposal, we dynamically control the splitting of Cooper pairs using a time-dependent gate voltage $V_g(t)$, as we explain below.

For energy levels positioned well inside the superconducting gap, the coherent dynamics of the dots due to the coupling to the superconductor can be described by the effective Hamiltonian [35–39],

$$\hat{H}(t) = \sum_{\ell\sigma} \epsilon_\ell(t) \hat{d}^\dagger_{\ell\sigma} \hat{d}_{\ell\sigma} - \left( \gamma \hat{d}^\dagger_S + \sum_\sigma \kappa \hat{d}^\dagger_{L\sigma} \hat{d}_{R\sigma} + \text{H.c.} \right), \tag{1}$$

where $\hat{d}^\dagger_{\ell\sigma}$ creates an electron with spin $\sigma = \uparrow, \downarrow$ in dot $\ell = L, R$, while $\hat{d}^\dagger_S \equiv (\hat{d}^\dagger_{L\downarrow}\hat{d}^\dagger_{R\uparrow} - \hat{d}^\dagger_{L\uparrow}\hat{d}^\dagger_{R\downarrow})/\sqrt{2}$ creates a two-electron spin-singlet state, which is delocalized across the two dots. Here, the (real) amplitudes for Cooper pair splitting and elastic cotunneling are denoted by $\gamma$ and $\kappa$, respectively, and $\epsilon_\ell(t)$ is the time-dependent energy level of each dot (relative to the chemical potential of the superconductor), which we tune by external gates to control the splitting of Cooper pairs and elastic cotunneling between the dots. Elastic cotunneling occurs mainly when the dot levels are aligned and the detuning $\delta = \epsilon_L - \epsilon_R$ vanishes. Similarly, Cooper pair splitting is on resonance when the doubly occupied dots have the same energy as the empty dots and the sum $\varepsilon = \epsilon_L + \epsilon_R$ vanishes. In general, Cooper pair splitting and elastic cotunneling lead to coherent oscillations with angular frequencies $\omega_\gamma = \sqrt{4\gamma^2 + \varepsilon^2}$ and $\omega_\kappa = \sqrt{4\kappa^2 + \delta^2}$, respectively, and both processes are suppressed as $\gamma^2/(\gamma^2 + \varepsilon^2/4)$ and $\kappa^2/(\kappa^2 + \delta^2/4)$ as we move away from the resonances. These suppression factors provide us with efficient experimental knobs to control the two types of processes. Thus, in the following, we consider the periodic driving protocol in Fig. 1(b), where Cooper pair splitting is tuned in ($\varepsilon = 0$) and out ($\varepsilon \gg \gamma$) of resonance, while elastic cotunneling is kept off resonance ($\delta \gg \kappa$). The duration of each phase is denoted by $T_j$, $j = 1, 2$, with $\hat{H}_j$ being the corresponding Hamiltonian, and $T = T_1 + T_2$ is the period of the drive.

With large negative voltages on the drains, the time evolution is governed by the Lindblad equation [40,41],

$$\frac{d}{dt}\hat{\rho}(t) = \mathcal{L}_j \hat{\rho}(t) = -\frac{i}{\hbar}[\hat{H}_j, \hat{\rho}(t)] + \mathcal{D}\hat{\rho}(t), \tag{2}$$

for each of the phases with Liouvillian $\mathcal{L}_j$, $j = 1, 2$, and $\hat{\rho}(t)$ is the density matrix of the dots, while the dissipator,

$$\mathcal{D}\hat{\rho}(t) = \Gamma \sum_{\sigma,\ell=L,R} \left( \mathcal{J}_{\ell\sigma}\hat{\rho}(t) - \frac{1}{2}\{\hat{\rho}(t), \hat{d}^\dagger_{\ell\sigma}\hat{d}_{\ell\sigma}\} \right), \tag{3}$$

describes the coupling to the drains. The jump operators $\mathcal{J}_{\ell\sigma}\hat{\rho}(t) \equiv \hat{d}_{\ell\sigma}\hat{\rho}(t)\hat{d}^\dagger_{\ell\sigma}$ describe the tunneling of single electrons to the drains with the rate $\Gamma$, and from hereon we take $\hbar$, $e = 1$. The simple form of the Lindblad dissipator is due to the large negative voltages on the drains. Our model can readily be refined according to a specific experiment, but to keep the discussion simple we do not include additional processes here.

*Driving protocol.*—We first consider our driving protocol in the weak coupling limit, $\Gamma \ll \gamma, \kappa$, suppressing elastic cotunneling using the off-resonance condition $\delta \gg \kappa$. In the first phase (1) [see Fig. 1(b)], Cooper pair splitting is tuned into resonance ($\varepsilon = 0$) for the time $T_1$. Ideally, during this phase, a Cooper pair is split between the dots, and we refer to $T_1$ as the loading time. In the second phase (2), Cooper pair splitting is turned off resonance ($\varepsilon \gg \gamma$) for the unloading time $T_2$, allowing the split Cooper pair to leave the dots via the drains. Since our protocol is based on turning Cooper pair splitting on and off, the steplike scheme is optimal for our purposes, and as shown in Fig. 1(a), it suffices to tune one of the levels in and out of resonance with the other. We now evaluate the drain currents to optimize the loading and unloading times.

Figures 1(c) and 1(d) show the average current for the periodic driving protocol obtained using a method described below. The current oscillates as a function of the loading time $T_1$ due to the coherent oscillations induced by Cooper pair splitting in the first phase. By contrast, the current increases monotonously as a function of $T_2$ until it saturates for $\Gamma T_2 \gtrsim 5$, reflecting that the unloading time is sufficiently long for the electrons to leave the dots. In this regime, the average current [the blue curve in Fig. 1(d)] can be captured by the simple expression

$$I = \frac{1}{T}\left( \sin^2(\gamma T_1) + \frac{1}{2}[\Gamma T_1 + (1 - e^{-\Gamma T_1})\cos(2\gamma T_1)] \right), \tag{4}$$

where the first term stems from the coherent oscillations for very small drain couplings, $\Gamma T_1 \ll 1$. Corresponding to

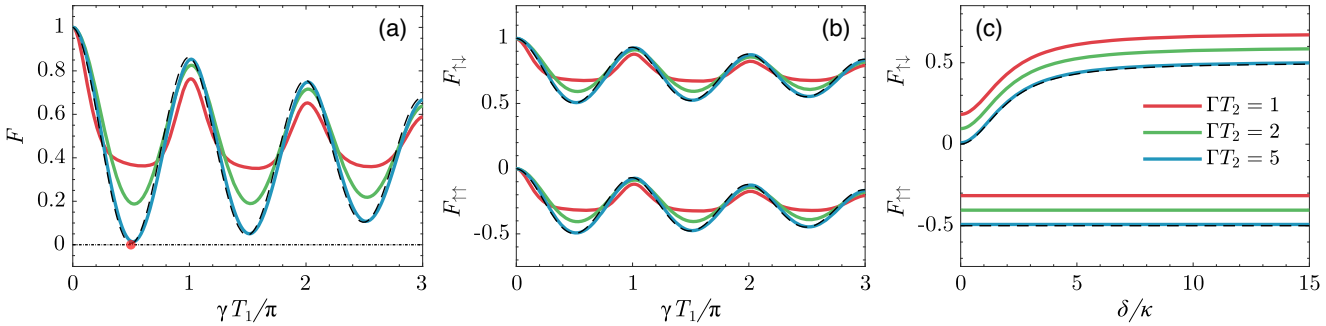


FIG. 2. Noise and spin correlations. (a) Fano factor as a function of the loading time $T_1$ for $\Gamma = 0.1\gamma$, $\gamma = \kappa$, $\delta = 100\kappa$, with $\varepsilon = 0$ in phase 1, and $\varepsilon = 100\gamma$ in phase 2. (b) Fano factors of the spin cross-correlations as a function of $T_1$ for the same settings as in (a). (c) Fano factors of the spin correlations as functions of $\delta$ with $\gamma T_1 = \pi/2$ and otherwise same parameters as in (a). The dashed lines in (a)–(c) are given by Eqs. (6)–(8), respectively.

this term, exactly one Cooper pair is split per period, if $\gamma T_1 = \pi(1/2 + m)$ for integer $m$. For finite couplings, the second term describes an unwanted leakage current during the first phase, which can be minimized by choosing a short loading time, $\Gamma T_1 \ll 1$. Thus, we find the optimal conditions $\gamma T_1 = \pi/2 \gg \Gamma T_1$ and $\Gamma T_2 \simeq 5$ shown with a red dot in Figs. 1(c) and 1(d), where on average one Cooper pair is split per period of the drive.

*Fluctuations.*—We now proceed with a refined analysis by investigating the noise in the outputs. To this end, we decompose the density matrix as $\hat{\rho}(t) = \sum_{\mathbf{n}} \hat{\rho}(\mathbf{n}, t)$, so that $P(\mathbf{n}, t) = \mathrm{tr}\{\hat{\rho}(\mathbf{n}, t)\}$ is the probability that $\mathbf{n} = (n_L, n_R)$ electrons have been collected in the drains during the time span $[0, t]$ [42,43]. The equations of motion for $\hat{\rho}(\mathbf{n}, t)$ are decoupled by introducing counting fields $\boldsymbol{\chi} = (\chi_L, \chi_R)$ via the transformation $\hat{\rho}(\boldsymbol{\chi}, t) = \sum_{\mathbf{n}} \hat{\rho}(\mathbf{n}, t) e^{i\mathbf{n}\cdot\boldsymbol{\chi}}$. We thereby obtain a generalized master equation for $\hat{\rho}(\boldsymbol{\chi}, t)$ with $\chi$-dependent Liouvillians $\mathcal{L}_j(\boldsymbol{\chi})$ by substituting $\mathcal{J}_{\ell\sigma} \to e^{i\chi_\ell}\mathcal{J}_{\ell\sigma}$ in Eq. (3) [38]. The moment generating function for the number of emitted electrons after $N$ periods now reads [44–46]

$$M(\boldsymbol{\chi}, N) = \mathrm{tr}\{\hat{\rho}(\boldsymbol{\chi}, NT)\} = \mathrm{tr}\{[\mathcal{U}(\boldsymbol{\chi}, T, 0)]^N \hat{\rho}_C(0)\}, \quad (5)$$

where the evolution operator for a time-dependent Liouvillian is given by a time-ordered exponential as $\mathcal{U}(\boldsymbol{\chi}, t, t_0) = \mathcal{T}\{\exp[\int_{t_0}^{t} \mathcal{L}(\boldsymbol{\chi}, t')dt']\}$, which we can explicitly evaluate for our piecewise constant protocol, and the cyclic state $\hat{\rho}_C(t)$ is determined by the eigenproblem $\mathcal{U}(\mathbf{0}, T + t, t)\hat{\rho}_C(t) = \hat{\rho}_C(t)$. The zero-frequency current correlators are then given by derivatives of the cumulant generating function $F(\boldsymbol{\chi}) = \lim_{N\to\infty} \ln[M(\boldsymbol{\chi}, N)]/NT$ as $\langle\langle I_L^k I_R^l \rangle\rangle = \partial_{i\chi_L}^k \partial_{i\chi_R}^l F(\boldsymbol{\chi})|_{\boldsymbol{\chi}=0}$. With these definitions, we can calculate the currents and their correlations using the methods from Refs. [47–49] and obtain simple expressions as those in Eqs. (4) and (6).

*Noise and Fano factor.*—Figure 2(a) shows the Fano factor, $F = \langle\langle I_\ell^2 \rangle\rangle / \langle\langle I_\ell \rangle\rangle$, $\ell = L, R$, of the noise in the drain electrodes, which for regular transport is suppressed below the Poisson value of one. Here, the Fano factor oscillates as a function of the loading time $T_1$, similarly to the average current in Figs. 1(c) and 1(d), and for long unloading times, $\Gamma T_2 \gg 1$, we find the simple expression

$$F = 1 - TI + \frac{2\Gamma T_1(1 + \Gamma T_1) + e^{-2\Gamma T_1} - 1}{8TI}, \quad (6)$$

corresponding to the dashed line in Fig. 2(a). For weak drain couplings, $\Gamma T_1 \ll 1$, the Fano factor reduces to $F = \cos^2(\gamma T_1)$, reflecting the coherent oscillations in the first phase. For larger couplings, the leakage current in the loading phase generates noise since more than one Cooper pair may be split during each period. Thus, we may minimize the noise by choosing $\gamma T_1 = \pi/2$ together with a long unloading time, $\Gamma T_2 \gg 1$, corresponding to the red dot in Fig. 2(a). There, the device produces exactly $N$ split Cooper pairs after $N$ periods, and it is noiseless in contrast to a static Cooper pair splitter. Deviations from the optimal conditions increase the noise due to cycle-missing events, in which no Cooper pair is split; however, the entanglement of each split pair is unaffected.

*Spin-current correlations.*—Next, we consider the cross-correlations between the spin currents in each drain, which play an important role for detecting the entanglement of the split Cooper pairs [50–53]. It is straightforward to include spin-dependent counting fields in Eq. (5), and in Fig. 2(b) we show the resulting cross-correlations, $F_{\sigma\sigma'} = \langle\langle I_{L\sigma} I_{R\sigma'} \rangle\rangle / \sqrt{\langle\langle I_{L\sigma} \rangle\rangle \langle\langle I_{R\sigma'} \rangle\rangle}$, as functions of the loading time $T_1$. The antiparallel spin currents are positively correlated, while parallel spins exhibit negative correlations, as expected for a split Cooper pair in a spin-singlet state. For long unloading times, $\Gamma T_2 \gg 1$, we find that the spin correlations Fig. 2(b) can be related to the Fano factor of the charge currents as

$$F_{\uparrow\downarrow} = 1 + F_{\uparrow\uparrow} = \frac{1}{2}(F + 1), \quad (7)$$

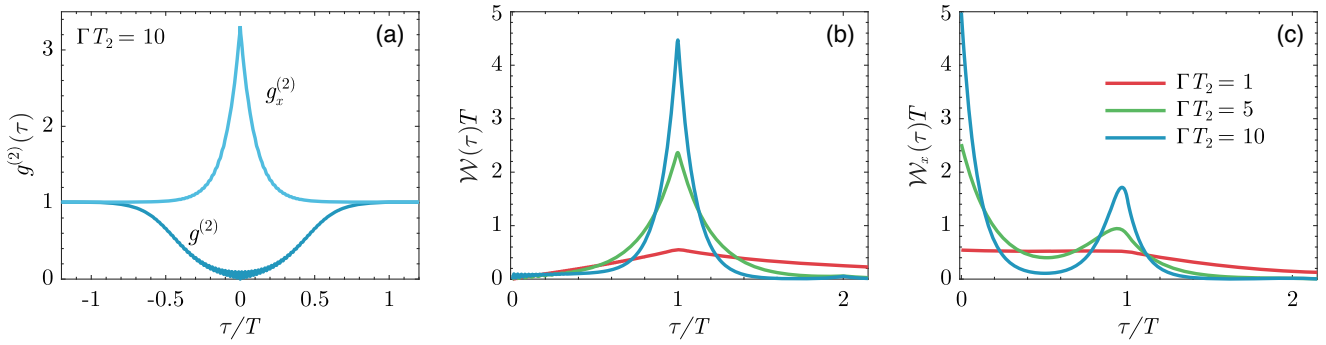


FIG. 3. Time-domain observables. (a) Autocorrelation ($g^{(2)}$) and cross-correlation ($g_x^{(2)}$) of the drain currents. (b) Distributions of waiting times between electrons tunneling into the same drain. (c) Distributions of waiting times between electrons tunneling into different drains. Parameters are $\gamma T_1 = \pi/2$, $\Gamma = 0.05\gamma$, $\kappa = \gamma$, $\delta = 20\kappa$ with $\varepsilon = 0$ in phase 1 and $\varepsilon = 20\gamma$ in phase 2.

making it possible to determine the spin correlations from noise measurements of the charge currents in the drains.

In Fig. 2(c), we consider the spin correlations as we tune elastic cotunneling into resonance. The negative correlations for parallel spins are essentially unchanged as elastic cotunneling is included. On the other hand, the positive correlations for antiparallel spins are gradually washed out by elastic cotunneling. We also consider a short loading time, $\Gamma T_1 \ll 1$, so that the leakage current is negligible during the first phase, and a long unloading time, $\Gamma T_2 \gg 1$, ensuring that at most one Cooper pair is split per period. Each uncorrelated period may then produce one of five outcomes: either no Cooper pair is split and no electrons reach the drain, or one Cooper pair is split and the two electrons tunnel into either of the two drains. We then approximate the generating function as

$$M(\boldsymbol{\chi}, N) \simeq \Big[1 - p + \frac{pq}{2}\big(e^{i(\chi_\uparrow^L + \chi_\downarrow^L)} + e^{i(\chi_\uparrow^R + \chi_\downarrow^R)}\big) + \frac{p(1-q)}{2}\big(e^{i(\chi_\uparrow^L + \chi_\downarrow^R)} + e^{i(\chi_\uparrow^R + \chi_\downarrow^L)}\big)\Big]^N, \quad (8)$$

where $p = \sin^2(\omega_\gamma T_1/2)\gamma^2/(\gamma^2 + \varepsilon^2/4)$ is the probability that a Cooper pair is split in the first phase, and $q = \frac{1}{2}\kappa^2/[\kappa^2 + (\Gamma^2 + \delta^2)/4]$ is the probability that the electrons leave via the same drain in the second phase due to elastic cotunneling. In Fig. 2(c), we show calculations of the spin correlations based on this approximation and find good agreement with the exact results. Furthermore, we find $F_{\uparrow\uparrow} = -p/2$ and $F_{\uparrow\downarrow} = 1 - p/2 - q$, which shows that, in this regime, $F_{\uparrow\uparrow}$ and $F_{\uparrow\downarrow}$ are sufficient to determine $p$ and $q$ and thus fully characterize the noise statistics.

*Time-domain analysis.*—Above, we focused on conventional low-frequency measurements. However, as in the experiment of Ref. [20], more information can be obtained by analyzing the fluctuations in the time domain. We thus consider the $g^{(2)}$ function of the currents [54,55],

$$g^{(2)}_{\ell\ell'}(\tau) = \int_0^T dt_0 \frac{\langle\!\langle \mathcal{J}_\ell \mathcal{U}(\mathbf{0}, t_0 + \tau, t_0)\mathcal{J}_{\ell'}\rangle\!\rangle_{t_0}}{\langle\!\langle \mathcal{J}_\ell\rangle\!\rangle_{t_0+\tau}\langle\!\langle \mathcal{J}_{\ell'}\rangle\!\rangle_{t_0}} P_{\ell'}(t_0), \quad (9)$$

with $\mathcal{J}_\ell \equiv \sum_\sigma \mathcal{J}_{\ell\sigma}$. Here, the probability density for the time that a tunneling event occurs reads $P_\ell(t) = \langle\!\langle \mathcal{J}_\ell\rangle\!\rangle_t / \int_0^T d\tau \langle\!\langle \mathcal{J}_\ell\rangle\!\rangle_\tau$, and $\langle\!\langle \mathcal{A}\rangle\!\rangle_t = \mathrm{tr}\{\mathcal{A}\hat{\rho}_C(t)\}$ is the expectation value of $\mathcal{A}$. In this definition, the correlations due to the periodic drive have been factored out.

Figure 3(a) shows the autocorrelations ($g^{(2)}$) and cross-correlations ($g_x^{(2)}$) of the drain currents. The autocorrelations are suppressed around $\tau = 0$, corresponding to the antibunching of electrons due to the Coulomb interactions on the dots. The cross-correlations, by contrast, exhibit a peak well above the uncorrelated value of one, showing how Cooper pair splitting leads to nearly simultaneous tunneling of electrons into different leads.

Information about the regularity of the dynamic Cooper pair splitter can be obtained from the waiting times between the tunneling events [20,56]. The distribution of waiting times can be expressed as [57–61]

$$\mathcal{W}_{\ell\ell'}(\tau) = \int_0^T dt_0 \frac{\langle\!\langle \mathcal{J}_\ell \mathcal{U}_\ell(t_0 + \tau, t_0)\mathcal{J}_{\ell'}\rangle\!\rangle_{t_0}}{\langle\!\langle \mathcal{J}_{\ell'}\rangle\!\rangle_{t_0}} P_{\ell'}(t_0), \quad (10)$$

where $\mathcal{U}_\ell(t, t_0) = \mathcal{T}\exp(\int_{t_0}^t [\mathcal{L}(\mathbf{0}, t') - \mathcal{J}_\ell]dt')$ is the time-evolution operator excluding electron tunneling into drain $\ell$. For $\ell = \ell'$, we obtain the distribution of waiting times between electrons tunneling into the same lead, while for $\ell \neq \ell'$, the distribution characterizes the waiting time between electrons tunneling into different leads.

Figures 3(b) and 3(c) show both types of distributions. With a long unloading time, $\Gamma T_2 \gg 1$, electrons tunneling into the same drain tend to be separated by the period of the drive due to the regular splitting of Cooper pairs. For shorter unloading times, the dots are not always emptied in the second phase, and the Cooper pair splitting becomes less regular. This picture is corroborated by the distributions for tunneling into different leads in Fig. 3(c). Here, the first peak at short waiting times corresponds to the

tunneling of electrons from the same split Cooper pair into different leads. In addition, the second peak corresponds to the waiting time between the last electron from one split Cooper pair and the first electron from the next split pair, and those are spaced by an interval, which is slightly shorter than the driving period.

*Experimental perspectives.*—To provide realistic parameters for our setup, we note that the superconducting gap can be around $\Delta \simeq 200\ \mu$eV [18] (corresponding to a temperature of 2.3 K), while the amplitudes for Cooper pair splitting and elastic cotunneling can be around $\gamma$, $\kappa \simeq 10\ \mu$eV. With a temperature of 100 mK, quasiparticle tunneling from outside the gap is then strongly suppressed. Moreover, with a detuning of $\delta = 100\ \mu$eV, elastic cotunneling can be suppressed by a factor of $\kappa^2/(\kappa^2+\delta^2) = 0.01$ compared to Cooper pair splitting. In addition, with tunneling rates being $\Gamma \simeq 1\ \mu$eV, we find $T_1 \simeq 1$ ns for the loading phase and $T_2 \simeq 10$ ns for the unloading phase, and the optimal driving frequency is then about 100 MHz with currents of about 10 pA.

*Conclusions.*—We have proposed a dynamic Cooper pair splitter that can generate a noiseless and regular flow of spin-entangled electrons, when operated under optimal conditions. Our proposals appears feasible in the light of recent experiments [20,56], and it may thus pave the way for the controlled generation of spin-entangled electrons. Moreover, additional control of the electron spins may be achieved with more elaborate pulse sequences [62], for instance, by using materials with strong spin-orbit coupling to generate effective, time-dependent magnetic fields [63]. Finally, entanglement witnesses based on current cross-correlations [52,53] may be used to certify the spin entanglement of the split Cooper pairs.

We thank N. Walldorf for his involvement at an early stage of the project and A. Ranni and V. F. Maisi for useful discussions. We acknowledge support from Aalto Science Institute and Academy of Finland through the Finnish Centre of Excellence in Quantum Technology (Projects No. 312057 and No. 312299) and Grants No. 308515 and No. 331737.

[1] M. Tinkham, *Introduction to Superconductivity* (Dover Publications, New York, 2004).
[2] G. B. Lesovik, T. Martin, and G. Blatter, Electronic entanglement in the vicinity of a superconductor, Eur. Phys. J. B **24**, 287 (2001).
[3] P. Recher, E. V. Sukhorukov, and D. Loss, Andreev tunneling, Coulomb blockade, and resonant transport of nonlocal spin-entangled electrons, Phys. Rev. B **63**, 165314 (2001).
[4] D. Beckmann, H. B. Weber, and H. v. Löhneysen, Evidence for Crossed Andreev Reflection in Superconductor-Ferromagnet Hybrid Structures, Phys. Rev. Lett. **93**, 197003 (2004).
[5] S. Russo, M. Kroug, T. M. Klapwijk, and A. F. Morpurgo, Experimental Observation of Bias-Dependent Nonlocal Andreev Reflection, Phys. Rev. Lett. **95**, 027002 (2005).
[6] L. Hofstetter, S. Csonka, J. Nygård, and C. Schönenberger, Cooper pair splitter realized in a two-quantum-dot Y-junction, Nature (London) **461**, 960 (2009).
[7] L. G. Herrmann, F. Portier, P. Roche, A. L. Yeyati, T. Kontos, and C. Strunk, Carbon Nanotubes as Cooper-Pair Beam Splitters, Phys. Rev. Lett. **104**, 026801 (2010).
[8] J. Wei and V. Chandrasekhar, Positive noise cross-correlation in hybrid superconducting and normal-metal three-terminal devices, Nat. Phys. **6**, 494 (2010).
[9] L. Hofstetter, S. Csonka, A. Baumgartner, G. Fülöp, S. d'Hollosy, J. Nygård, and C. Schönenberger, Finite-Bias Cooper Pair Splitting, Phys. Rev. Lett. **107**, 136801 (2011).
[10] J. Schindele, A. Baumgartner, and C. Schönenberger, Near-Unity Cooper Pair Splitting Efficiency, Phys. Rev. Lett. **109**, 157002 (2012).
[11] L. G. Herrmann, P. Burset, W. J. Herrera, F. Portier, P. Roche, C. Strunk, A. Levy Yeyati, and T. Kontos, Spectroscopy of non-local superconducting correlations in a double quantum dot, arXiv:1205.1972.
[12] A. Das, R. Ronen, M. Heiblum, D. Mahalu, A. V. Kretinin, and H. Shtrikman, High-efficiency Cooper pair splitting demonstrated by two-particle conductance resonance and positive noise cross-correlation, Nat. Commun. **3**, 1165 (2012).
[13] G. Fülöp, S. d'Hollosy, A. Baumgartner, P. Makk, V. A. Guzenko, M. H. Madsen, J. Nygård, C. Schönenberger, and S. Csonka, Local electrical tuning of the nonlocal signals in a Cooper pair splitter, Phys. Rev. B **90**, 235412 (2014).
[14] Z. B. Tan, D. Cox, T. Nieminen, P. Lähteenmäki, D. Golubev, G. B. Lesovik, and P. J. Hakonen, Cooper Pair Splitting by Means of Graphene Quantum Dots, Phys. Rev. Lett. **114**, 096602 (2015).
[15] G. Fülöp, F. Domínguez, S. d'Hollosy, A. Baumgartner, P. Makk, M. H. Madsen, V. A. Guzenko, J. Nygård, C. Schönenberger, A. Levy Yeyati, and S. Csonka, Magnetic Field Tuning and Quantum Interference in a Cooper Pair Splitter, Phys. Rev. Lett. **115**, 227003 (2015).
[16] I. V. Borzenets, Y. Shimazaki, G. F. Jones, M. F. Craciun, S. Russo, M. Yamamoto, and S. Tarucha, High efficiency CVD graphene-lead (Pb) cooper pair splitter, Sci. Rep. **6**, 23051 (2016).
[17] L. E. Bruhat, T. Cubaynes, J. J. Viennot, M. C. Dartiailh, M. M. Desjardins, A. Cottet, and T. Kontos, Circuit QED with a quantum-dot charge qubit dressed by Cooper pairs, Phys. Rev. B **98**, 155313 (2018).
[18] Z. B. Tan, A. Laitinen, N. S. Kirsanov, A. Galda, V. M. Vinokur, M. Haque, A. Savin, D. S. Golubev, G. B. Lesovik, and P. J. Hakonen, Thermoelectric current in a graphene Cooper pair splitter, Nat. Commun. **12**, 138 (2021).
[19] P. Pandey, R. Danneau, and D. Beckmann, Ballistic Graphene Cooper Pair Splitter, Phys. Rev. Lett. **126**, 147701 (2021).
[20] A. Ranni, F. Brange, E. T. Mannila, C. Flindt, and V. F. Maisi, Real-time observation of Cooper pair splitting showing strong non-local correlations, Nat. Commun. **12**, 6358 (2021).

[21] M. D. Blumenthal, B. Kaestner, L. Li, S. Giblin, T. J. B. M. Janssen, M. Pepper, D. Anderson, G. Jones, and D. A. Ritchie, Gigahertz quantized charge pumping, Nat. Phys. **3**, 343 (2007).
[22] G. Fève, A. Mahé, J.-M. Berroir, T. Kontos, B. Plaçais, D. C. Glattli, A. Cavanna, B. Etienne, and Y. Jin, An on-demand coherent single-electron source, Science **316**, 1169 (2007).
[23] E. Bocquillon, V. Freulon, J.-M Berroir, P. Degiovanni, B. Plaçais, A. Cavanna, Y. Jin, and G. Fève, Coherence and indistinguishability of single electrons emitted by independent sources, Science **339**, 1054 (2013).
[24] J. Dubois, T. Jullien, F. Portier, P. Roche, A. Cavanna, Y. Jin, W. Wegscheider, P. Roulleau, and D. C. Glattli, Minimal-excitation states for electron quantum optics using levitons, Nature (London) **502**, 659 (2013).
[25] T. Jullien, P. Roulleau, B. Roche, A. Cavanna, Y. Jin, and D. C. Glattli, Quantum tomography of an electron, Nature (London) **514**, 603 (2014).
[26] J. D. Fletcher, P. See, H. Howe, M. Pepper, S. P. Giblin, J. P. Griffiths, G. A. C. Jones, I. Farrer, D. A. Ritchie, T. J. B. M. Janssen, and M. Kataoka, Clock-Controlled Emission of Single-Electron Wave Packets in a Solid-State Circuit, Phys. Rev. Lett. **111**, 216807 (2013).
[27] L. Fricke, M. Wulf, B. Kaestner, F. Hohls, P. Mirovsky, B. Mackrodt, R. Dolata, T. Weimann, K. Pierz, U. Siegner, and H. W. Schumacher, Self-Referenced Single-Electron Quantized Current Source, Phys. Rev. Lett. **112**, 226803 (2014).
[28] N. Ubbelohde, F. Hohls, V. Kashcheyevs, T. Wagner, L. Fricke, B. Kstner, K. Pierz, H. W. Schumacher, and R. J. Haug, Partitioning of on-demand electron pairs, Nat. Nanotechnol. **10**, 46 (2015).
[29] D. M. T. van Zanten, D. M. Basko, I. M. Khaymovich, J. P. Pekola, H. Courtois, and C. B. Winkelmann, Single Quantum Level Electron Turnstile, Phys. Rev. Lett. **116**, 166801 (2016).
[30] J. P. Pekola, O.-P. Saira, V. F. Maisi, A. Kemppinen, M. Möttönen, Yu. A. Pashkin, and D. V. Averin, Single-electron current sources: Toward a refined definition of the ampere, Rev. Mod. Phys. **85**, 1421 (2013).
[31] C. W. J. Beenakker, M. Titov, and B. Trauzettel, Optimal Spin-Entangled Electron-Hole Pair Pump, Phys. Rev. Lett. **94**, 186804 (2005).
[32] P. Samuelsson and M. Büttiker, Dynamic generation of orbital quasiparticle entanglement in mesoscopic conductors, Phys. Rev. B **71**, 245317 (2005).
[33] A. V. Lebedev, G. B. Lesovik, and G. Blatter, Generating spin-entangled electron pairs in normal conductors using voltage pulses, Phys. Rev. B **72**, 245314 (2005).
[34] P. P. Hofer and M. Büttiker, Emission of time-bin entangled particles into helical edge states, Phys. Rev. B **88**, 241308 (R) (2013).
[35] O. Sauret, D. Feinberg, and T. Martin, Quantum master equations for the superconductor-quantum dot entangler, Phys. Rev. B **70**, 245313 (2004).
[36] J. Eldridge, M. G. Pala, M. Governale, and J. König, Superconducting proximity effect in interacting double-dot systems, Phys. Rev. B **82**, 184507 (2010).
[37] B. Hiltscher, M. Governale, J. Splettstoesser, and J. König, Adiabatic pumping in a double-dot Cooper-pair beam splitter, Phys. Rev. B **84**, 155403 (2011).
[38] N. Walldorf, F. Brange, C. Padurariu, and C. Flindt, Noise and full counting statistics of a Cooper pair splitter, Phys. Rev. B **101**, 205422 (2020).
[39] In our effective low-energy description, we assume that the Coulomb interactions on the quantum dots are so strong that they cannot be doubly occupied. Moreover, the spacing of the single-particle states is so large that only a single level of each dot participates in the quantum transport. Those levels are kept well inside the superconducting gap, so that quasiparticle tunneling from outside the gap is strongly suppressed at low temperatures.
[40] H.-P. Breuer and F. Petruccione, *The Theory of Open Quantum Systems* (Oxford University Press, New York, 2003).
[41] B. L. Hazelzet, M. R. Wegewijs, T. H. Stoof, and Yu. V. Nazarov, Coherent and incoherent pumping of electrons in double quantum dots, Phys. Rev. B **63**, 165313 (2001).
[42] M. B. Plenio and P. L. Knight, The quantum-jump approach to dissipative dynamics in quantum optics, Rev. Mod. Phys. **70**, 101 (1998).
[43] Yu. Makhlin, G. Schön, and A. Shnirman, Quantum-state engineering with Josephson-junction devices, Rev. Mod. Phys. **73**, 357 (2001).
[44] F. Pistolesi, Full counting statistics of a charge shuttle, Phys. Rev. B **69**, 245409 (2004).
[45] M. Albert, C. Flindt, and M. Büttiker, Accuracy of the quantum capacitor as a single-electron source, Phys. Rev. B **82**, 041407(R) (2010).
[46] E. Potanina, K. Brandner, and C. Flindt, Optimization of quantized charge pumping using full counting statistics, Phys. Rev. B **99**, 035437 (2019).
[47] C. Flindt, T. Novotný, and A.-P. Jauho, Full counting statistics of nano-electromechanical systems, Europhys. Lett. **69**, 475 (2005).
[48] C. Flindt, T. Novotný, A. Braggio, M. Sassetti, and A.-P. Jauho, Counting Statistics of Non-Markovian Quantum Stochastic Processes, Phys. Rev. Lett. **100**, 150601 (2008).
[49] C. Flindt, T. Novotný, A. Braggio, and A.-P. Jauho, Counting statistics of transport through Coulomb blockade nanostructures: High-order cumulants and non-Markovian effects, Phys. Rev. B **82**, 155407 (2010).
[50] S. Kawabata, Test of Bell's Inequality using the Spin Filter Effect in Ferromagnetic Semiconductor Microstructures, J. Phys. Soc. Jpn. **70**, 1210 (2001).
[51] O. Malkoc, C. Bergenfeldt, and P. Samuelsson, Full counting statistics of generic spin entangler with quantum dot-ferromagnet detectors, Europhys. Lett. **105**, 47013 (2014).
[52] P. Busz, D. Tomaszewski, and J. Martinek, Spin correlation and entanglement detection in Cooper pair splitters by current measurements using magnetic detectors, Phys. Rev. B **96**, 064520 (2017).
[53] F. Brange, O. Malkoc, and P. Samuelsson, Minimal Entanglement Witness from Electrical Current Correlations, Phys. Rev. Lett. **118**, 036804 (2017).
[54] H. J. Carmichael, S. Singh, R. Vyas, and P. R. Rice, Photoelectron waiting times and atomic state reduction in resonance fluorescence, Phys. Rev. A **39**, 1200 (1989).
[55] C. Emary, C. Pöltl, A. Carmele, J. Kabuss, A. Knorr, and T. Brandes, Bunching and antibunching in electronic transport, Phys. Rev. B **85**, 165417 (2012).

[56] F. Brange, A. Schmidt, J. C. Bayer, T. Wagner, C. Flindt, and R. J. Haug, Controlled emission time statistics of a dynamic single-electron transistor, Sci. Adv. **7**, eabe0793 (2021).
[57] T. Brandes, Waiting times and noise in single particle transport, Ann. Phys. (Berlin) **17**, 477 (2008).
[58] M. Albert, C. Flindt, and M. Büttiker, Distributions of Waiting Times of Dynamic Single-Electron Emitters, Phys. Rev. Lett. **107**, 086805 (2011).
[59] E. Potanina and C. Flindt, Electron waiting times of a periodically driven single-electron turnstile, Phys. Rev. B **96**, 045420 (2017).
[60] N. Walldorf, C. Padurariu, A.-P. Jauho, and C. Flindt, Electron Waiting Times of a Cooper Pair Splitter, Phys. Rev. Lett. **120**, 087701 (2018).
[61] K. Wrześniewski and I. Weymann, Current cross-correlations and waiting time distributions in Andreev transport through Cooper pair splitters based on a triple quantum dot system, Phys. Rev. B **101**, 155409 (2020).
[62] J. R. Petta, A. C. Johnson, J. M. Taylor, E. A. Laird, A. Yacoby, M. D. Lukin, C. M. Marcus, M. P. Hanson, and A. C. Gossard, Coherent manipulation of coupled electron spins in semiconductor quantum dots, Science **309**, 2180 (2005).
[63] C. Flindt, A. S. Sørensen, and K. Flensberg, Spin-Orbit Mediated Control of Spin Qubits, Phys. Rev. Lett. **97**, 240501 (2006).